THE ASTROPHYSICAL JOURNAL, 418:570–578, 1993 December 1


# LINEAR EVOLUTION OF THE GRAVITATIONAL POTENTIAL: A NEW APPROXIMATION FOR THE NONLINEAR EVOLUTION OF LARGE-SCALE STRUCTURE

TEREASA G. BRAINERD,[1,2] ROBERT J. SCHERRER,[3] AND JENS V. VILLUMSEN[1]
*Received 1992 December 16; accepted 1993 June 7*

## ABSTRACT

Using a full nonlinear numerical gravitational clustering simulation with $\Omega = 1$ cold dark matter and Zel'dovich initial conditions, we show that the gravitational potential evolves very little up to the present on length scales $\geq 1.25\ h^{-1}$ Mpc. We present a new approximation for the nonlinear evolution of large-scale structure, in which the gravitational potential field is assumed to remain constant up to the present, but the matter obeys the usual nonlinear equations of motion in this potential field. We calculate evolved density fields using this approximation and compare them to the Zel'dovich approximation and a full nonlinear evolution. At late times, the accuracy of our results lies between the Zel'dovich approximation and a full nonlinear evolution.

*Subject headings:* galaxies: clustering — large-scale structure of universe — methods: numerical

## 1. INTRODUCTION

In principle, the problem of calculating the evolution of the large-scale structure of the universe is a simple exercise in Newtonian dynamics. In practice, of course, the nonlinear evolution of the density field requires a numerical gravitational clustering simulation. Although a full numerical simulation is the most accurate and useful technique for calculating large-scale structure, there are several reasons for exploring analytic approximations for the nonlinear evolution of the density field. First of all, such techniques may provide insight into the nature of the evolution which cannot be gleaned from endless computer simulations. For example, the Zel'dovich approximation (Zel'dovich 1970) demonstrates analytically the formation of walls and filaments in gravitational clustering. Second, such techniques may provide a faster and easier-to-use method for calculating the evolution of large-scale structure.

A number of such techniques have already been developed. The application of perturbation theory leads to the well-known linear evolution equations; this technique can also be extended to second-order to provide an equation for the evolution of skewness (Peebles 1980); of course, these approximations fail when $\delta\rho/\rho > 1$. Other approximations include the Zel'dovich approximation (Zel'dovich 1970), in which the motion of each particle is determined entirely by its initial (Lagrangian) potential, the second-order extension of the Zel'dovich approximation (Gramann 1993), the frozen-flow approximation (Matarrese et al. 1992), in which the velocity of each particle is given by its local linear value, the lognormal approximation (Coles & Jones 1991), which involves a local mapping of the density field via an exponential transformation, and the adhesion model (Gurbatov, Saichev, & Shandarin 1989) in which the particles move according to the Zel'dovich equations of motion, but with the addition of viscosity to allow the particles to stick together and form pancakes. A somewhat different problem has been addressed by Nusser & Deckel (1992) and Weinberg (1992), who have developed approximations to extrapolate the current density field backwards to obtain the initial conditions.

Here we introduce a new semianalytical approximation, which we shall call linear evolution of the potential (LEP). In this approximation, we assume that the potential field obeys the linear evolution equations (i.e., it is constant for $\Omega = 1$), and the particles obey the standard equations of motion in this potential. In a sense, this approximation is an extension of the Zel'dovich approximation. In the Zel'dovich approximation, the Lagrangian potential is taken to be constant, while in our approximation, the Eulerian potential is constant. In § 2, we provide a complete description of our approximation and also demonstrate, using a full nonlinear gravitational clustering simulation, that the gravitational potential is indeed nearly constant up to the present on length scales $\sim 1.25\ h^{-1}$ Mpc. Also in § 2 we compare the results of our LEP approximation to the predictions of the Zel'dovich approximation and to a full nonlinear simulation and derive several analytic results. Our conclusions are presented in § 3. Our approximation resembles the frozen-flow approximation, and indeed some of our results in § 2 can be taken as a justification for this approximation as well. We explain briefly in § 2 the similarities and differences between these two approaches.

## 2. LINEAR EVOLUTION OF THE POTENTIAL

The equations of motion for the matter in the universe are conventionally written in terms of the dimensionless density contrast $\delta(\boldsymbol{x})$, defined as

$$\delta(\boldsymbol{x}) = [\rho(\boldsymbol{x}) - \bar{\rho}]/\bar{\rho}\ , \tag{2.1}$$

where $\rho(\boldsymbol{x})$ is the matter density at the comoving point $\boldsymbol{x}$, and $\bar{\rho}$ is the mean matter density. Neglecting pressure, the equations governing the evolution of the density are the continuity equation:

$$\frac{\partial\rho}{\partial t} + 3\,\frac{\dot{a}}{a}\,\rho + \frac{1}{a}\,\nabla\cdot(\rho\boldsymbol{v}) = 0\ , \tag{2.2}$$

the Euler equation:

$$\frac{d\boldsymbol{v}}{dt} + \frac{\dot{a}}{a}\,\boldsymbol{v} = \frac{-\nabla\phi}{a}\ , \tag{2.3}$$

[1] Department of Astronomy, The Ohio State University, Columbus, OH 43210.
[2] Theoretical Astrophysics 130–33, California Institute of Technology, Pasadena, CA 91125.
[3] Department of Physics, The Ohio State University, Columbus, OH 43210.

and the Poisson equation:

$$\nabla^2\phi = 4\pi G a^2 \bar{\rho}\delta \,. \tag{2.4}$$

In these equations, $a$ is the scale factor, $\phi$ is the peculiar gravitational potential, $v = a(dx/dt)$ is the proper peculiar velocity, and $d/dt$ is the convective derivative, i.e., the derivative measured at a point moving with the flow; it is related to the derivative $\partial/\partial t$ measured at a fixed Eulerian point by $d/dt = \partial/\partial t + (v/a)\cdot\nabla$. For $\Omega = 1$ in the linear regime in the matter-dominated era, $\delta \propto a$ and $\bar{\rho} \propto a^{-3}$, so equation (2.4) indicates that $\phi$ is constant.

Note that we can rewrite equation (2.4) in terms of the Fourier components $\hat{\delta}(k)$ and $\hat{\phi}(k)$:

$$\hat{\phi}(k) = -4\pi G a^2 \bar{\rho}\,\frac{\hat{\delta}(k)}{k^2} \,. \tag{2.5}$$

Because of the $k^{-2}$ factor on the right-hand side, the potential weights the long-wavelength modes more strongly than does the density field. In the standard cold dark matter model with a Zel'dovich power spectrum, the longer wavelength modes go nonlinear at a later time than the shorter wavelength modes, so we might expect the potential on a given length scale to be described by linear perturbation theory long after the density field is strongly nonlinear on that length scale. As noted above, this implies that $\phi$ remains nearly constant well into the nonlinear regime.

To test this hypothesis, we have run a gravitational clustering simulation of a standard cold dark matter universe ($\Omega = 1$, $\Lambda = 0$, $h = \frac{1}{2}$) using a particle mesh (PM) gravitational clustering code (Villumsen 1989). The simulation volume was 80 $h^{-1}$ Mpc (comoving) on a side; $128^3$ particles and $256^3$ grid cells were used. We characterize various epochs in the simulation by the linear bias factor $b$, which we define as the inverse of the rms mass fluctuation in a spherical top hat of radius 8 $h^{-1}$ Mpc in the linear regime,

$$\frac{1}{b} \equiv \left\langle \left(\frac{\delta M}{M}\right)^2 \right\rangle^{1/2}_{(8\ h^{-1}\ \mathrm{Mpc})} \,. \tag{2.6}$$

(See, for example, Bardeen et al. 1986). In the nonlinear regime, we take $1/b \propto a$, so equation (2.6) is no longer valid. The simulation began at $b = 30$, which we define to be an expansion factor, $a$, of 1. The simulation was evolved through 30 expansion factors and ended at $b = 1.0$, corresponding to an expansion factor, $a$, of 30. If we define $b = 1.0$ to be "today" (i.e., redshift of $z = 0$), then the beginning of the simulation corresponds to a redshift of $z = 29$. Using cloud-in-cell (CIC) interpolation (see, for example, Efstathiou et al. 1985) the potential and density fields at various epochs in the simulation were determined on a $64^3$ grid (i.e., a coarse grid whose grid cells are 4 times the length of the grid cells used in the simulation). The length of a grid cell on this coarse grid is 1.25 $h^{-1}$ Mpc. The initial density contrast $\delta_i$ and initial potential field $\phi_i$ were randomly sampled on the $64^3$ grid (1% of the grid cells were used) and then compared with the values of $\delta$ and $\phi$ in the same grid cells at later epochs of the simulation. The results are displayed in Figures 1 and 2.

While there is still some obvious correlation between the initial and final values of $\delta$ at $b = 10$ ($a = 3$), this correlation has dissolved by $b = 1.0$ ($a = 30$). (The lower cutoff on $\delta/a$ corresponds to empty cells in the simulation.) The potential, on

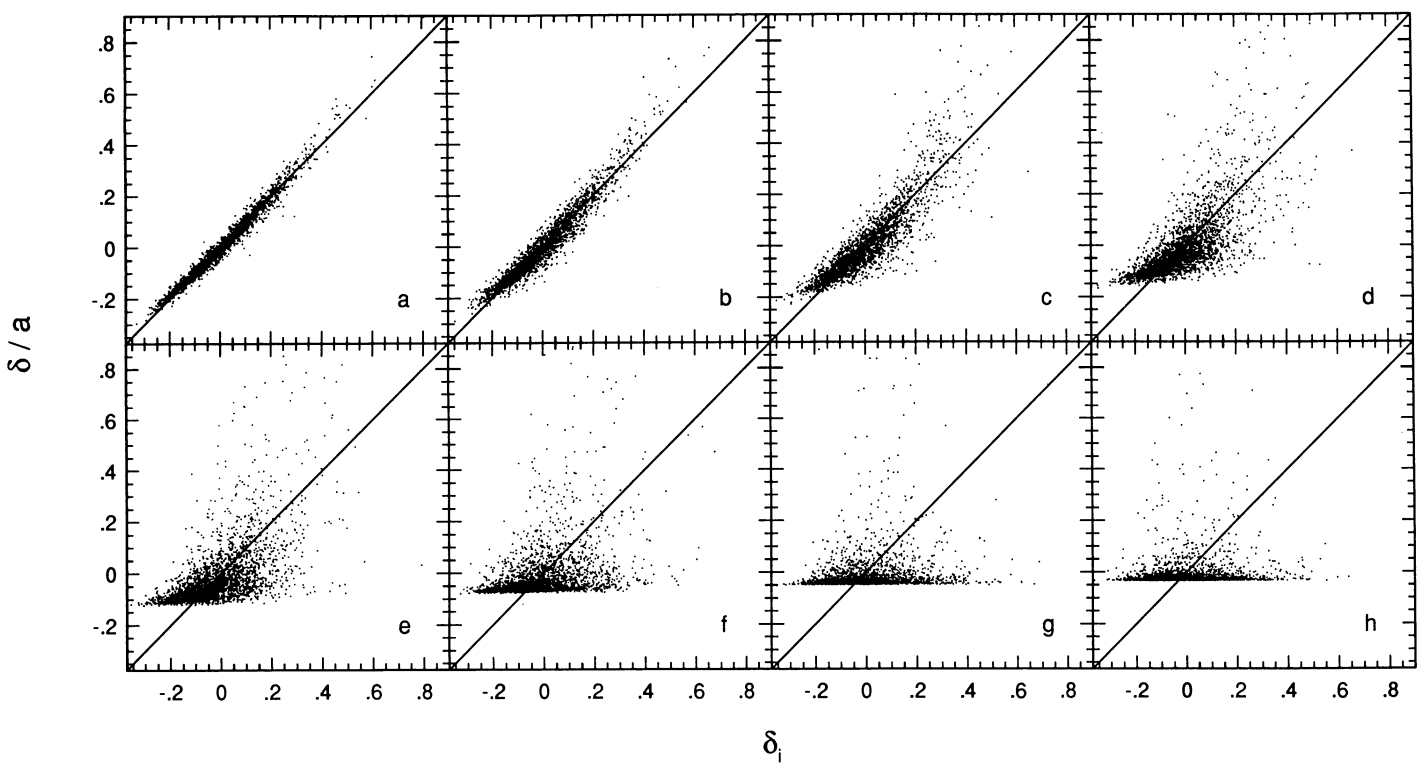


FIG. 1.—The initial density contrast, $\delta_i$, at a grid point in an $\Omega = 1$ adiabatic Harrison-Zel'dovich CDM gravitational clustering simulation compared to the density contrast divided by the expansion factor, $\delta/a$, at later epochs in the simulation, at the same grid point. Densities are sampled on a $64^3$ grid (length of a grid cell $= 1.25\ h^{-1}$ Mpc), and the results from a random 1% of the grid cells are shown. Panels (*a*)–(*h*) represent expansion factors $a = 1.5$, 2.0, 3.0, 5.0, 7.0, 12.0, 20.0, and 30.0 (corresponding to linear bias factors, $b = 20.0$, 15.0, 10.0, 6.0, 4.3, 2.5, 1.5, and 1.0). Grid points for which $\delta = \delta_i a$ fall along the straight line shown in the figures.

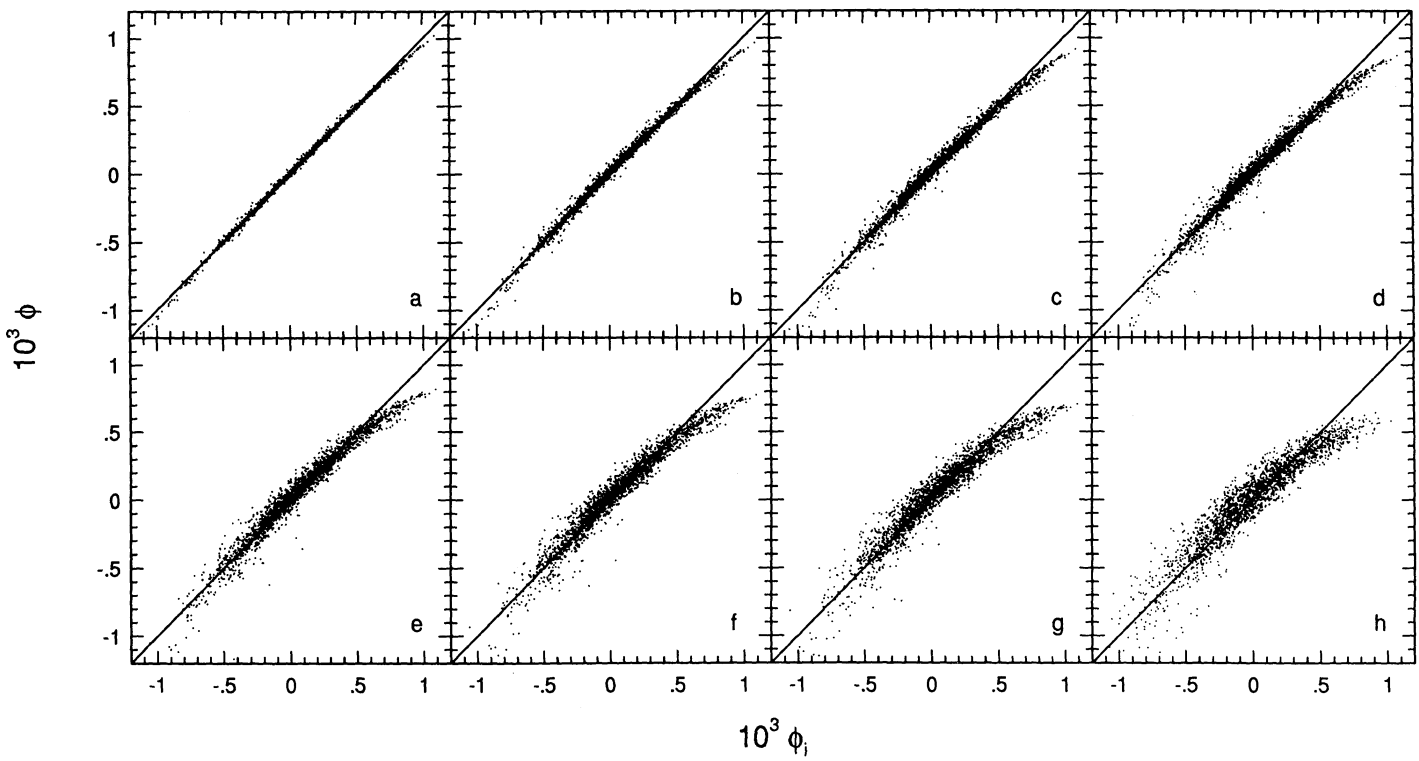


FIG. 2.—The initial peculiar gravitational potential field, $\phi_i$, at a grid point in an $\Omega = 1$ adiabatic Harrison-Zel'dovich CDM gravitational clustering simulation compared to the peculiar gravitational potential field, $\phi$, at later epochs in the simulation at the same grid point. Potentials are sampled on a $64^3$ grid (length of a grid cell $= 1.25\,h^{-1}$ Mpc), and the results from a random 1% of the grid cells are shown. Panels (*a*)–(*h*) represent expansion factors $a = 3.0$, 5.0, 7.0, 9.0, 12.0, 15.0, 20.0, and 30.0 (corresponding to linear bias factors, $b$, of 10.0, 6.0, 4.3, 3.3, 2.5, 2.0, 1.5, and 1.0). Grid points for which $\phi = \phi_i$ fall along the straight line shown in the figures.

the other hand, is well described by linear evolution ($\phi$ = constant) up to $b = 1.0$. While there is some artificial softening of the potential (because we are using a PM code), we sample on scales a factor of 4 larger than the grid cutoff. The potential deviates from the constant value predicted by linear evolution at both ends of the graph, i.e., for both the largest negative and largest positive values of the initial potential $\phi_i$. The deviation from linear behavior for large negative $\phi_i$ occurs because linear theory breaks down in the deepest potential wells; these deep potential wells produce a larger negative potential than can be produced by naively applying linear theory. The deviation from linear behavior at large positive $\phi_i$ arises from the fact that our density field is nonnegative, so that $\delta > -1$. This physical lower bound on $\delta$ causes linear theory to break down in the lowest-density regions, which correspond to the largest positive values of $\phi$.

Of course, it is not $\phi$, but $\nabla\phi$ which enters into the equations of motion (eq. [2.3]). Therefore, we have also examined the correlation between the initial and evolved values of $\nabla\phi$ in our simulation. We examined a single component of $\nabla\phi$ ($d\phi/dx$), calculated on a cell by taking the difference between the potential on the two cells on opposite sides of the given cell. The value of $d\phi/dx$ at later epochs as a function of the initial linear value of $d\phi/dx$ is shown in Figure 3. The correlation is not as strong as it is for $\phi$; this is to be expected because the Fourier components of $\nabla\phi$ scale as one higher power of $k$ than does $\hat{\phi}(k)$, and $\nabla\phi$ is therefore more sensitive than $\phi$ to nonlinear modes. However, there is still an obvious correlation between the initial value of $d\phi/dx$ and its value at later epochs, much stronger than the correlation between the initial and final density fields.

The fact that the potential and its gradient are roughly described by linear evolution down to the present suggests an obvious approximation for the evolution of large-scale structure: we take $\phi$ to be constant, and evolve the density field in this constant potential field using the full nonlinear equations of motion. In essence, we retain equations (2.2) and (2.3), but modify equation (2.4), simply retaining the initial potential field as the potential field at all later times. This approximation is in some sense a generalization of the Zel'dovich approximation. In the Zel'dovich approximation, the Lagrangian potential field is constant: each particle sees the potential appropriate to its initial position. In our approximation, the Eulerian potential is constant; each particle experiences a changing potential as it moves through space, but the potential at a fixed Eulerian coordinate is constant.

Our approach is also somewhat similar to the frozen-flow approximation of Matarrese et al. (1992). In that approximation, the Eulerian potential is held constant, and each particle takes the instantaneous velocity appropriate for its local potential in linear theory; the particle has no memory of its previous velocity. In our approximation, the velocity is determined by Newtonian dynamics. In order from the simplest approximation to the most complex (and closest to a full gravitational clustering simulation), we have the Zel'dovich approximation, the frozen-flow approximation, and our linear evolution of the potential.

We have evolved a CDM simulation of length $80\,h^{-1}$ Mpc on a side consisting of $32^3$ particles in a $64^3$ grid using a full numerical (PM) simulation, the Zel'dovich approximation, and our linear evolution of the potential (LEP) approximation. All three simulations were begun at $b = 23$ with identical initial

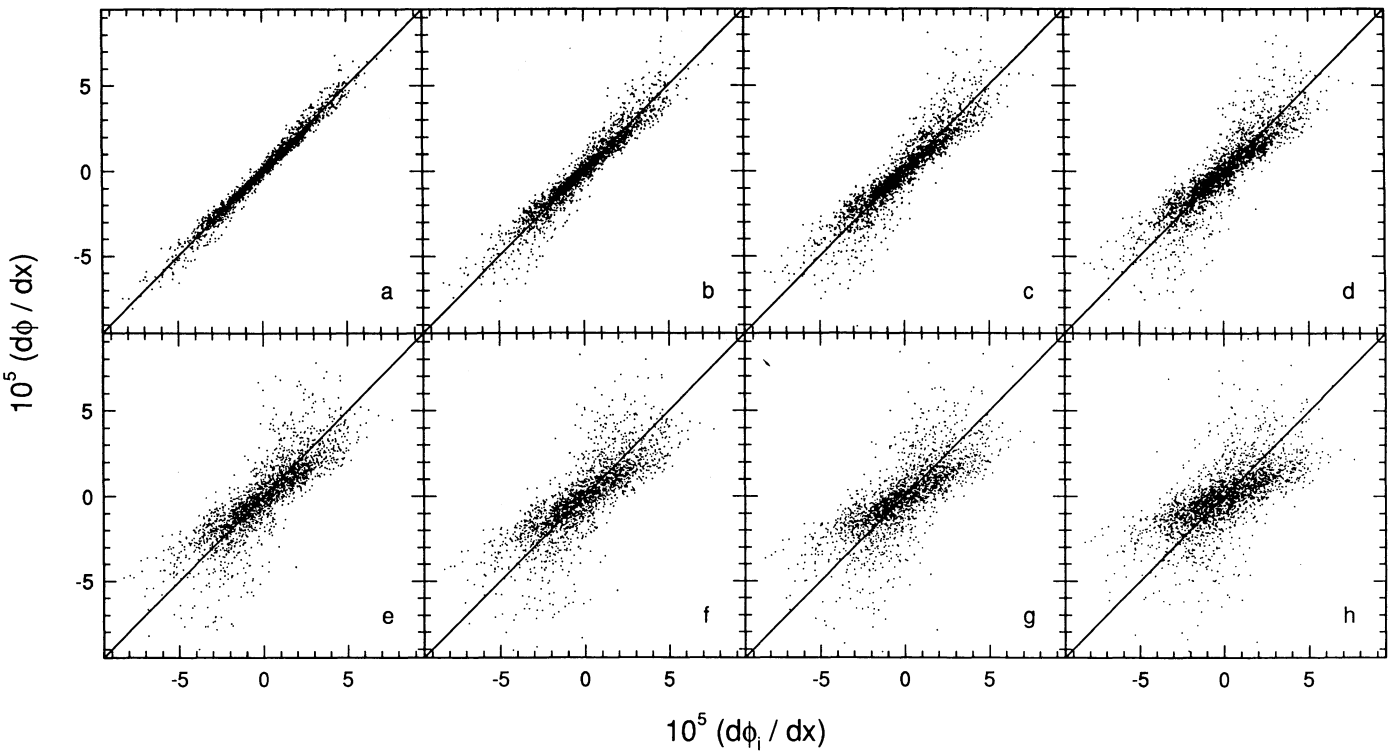


FIG. 3.—A single component of the gradient of the initial peculiar gravitational potential field, $d\phi_i/dx$, at a grid point in an $\Omega = 1$ adiabatic Harrison-Zel'dovich CDM gravitational clustering simulation compared to $d\phi/dx$ at later epochs in the simulation at the same grid point. Potential gradients are sampled on a $64^3$ grid (length of a grid cell $= 1.25\ h^{-1}$ Mpc), and the results from a random 1% of the grid cells are shown. Panels (*a*)–(*h*) represent expansion factors $a = 3.0$, 5.0, 7.0, 9.0, 12.0, 15.0, 20.0, and 30.0 (corresponding to linear bias factors, $b$, of 10.0, 6.0, 4.3, 3.3, 2.5, 2.0, 1.5, and 1.0). Grid points for which $d\phi/dx = d\phi_i/dx$ fall along the straight line shown in the figures.

conditions. In Figure 4, we present slices of these simulations evolved down to $b = 1$. Figure 4*a* is the full numerical simulation, Figure 4*b* is the Zel'dovich approximation, and Figure 4*c* is the linear evolution of the potential. Visually, our LEP approximation gives much better results than the Zel'dovich approximation. The Zel'dovich approximation gives poor results when evolved to the present because shell crossing has already occurred, and the particles are streaming out of the caustics. Our approximation reproduces the formation of knots and filaments in roughly the same locations as in the full numerical simulation. The main defect of our LEP approximation is the failure to reproduce the highest-density peaks in the full numerical simulation. This is to be expected, since the high-density peaks can produce potentials larger than the result obtained from simple linear evolution, allowing much denser structures to form.

Although the visual similarity between our approximation and the nonlinear evolution is obvious, we have also used several statistical measures to compare these two approaches. We first examined the cross-correlation, defined (for two density fields $X$ and $Y$) to be

$$S = \langle (X_i - \bar{X})(Y_i - \bar{Y}) \rangle / \sigma_x \sigma_y , \qquad (2.7)$$

where $X_i$ and $Y_i$ are the densities in the $i$th pixels of the two density fields, $\sigma_x$ and $\sigma_y$ are the rms fluctuations in the two fields, and we average over all pixels in the two density fields. This statistic was used by Coles, Melott, & Shandarin (1992) to compare a number of analytic approximations for nonlinear evolution. (Note that we compare only the unsmoothed density fields, while Coles et al. examined both smoothed and unsmoothed fields.) Using this statistic, we find, paradoxically, that our LEP approximation gives *worse* agreement with the full numerical simulation than does the Zel'dovich approximation. A similar effect is seen by Matarrese et al. (1992); despite the fact that their frozen-flow approximation is visually more similar to the full numerical simulation than is the Zel'dovich approximation, the correlation between the evolved densities in the numerical simulation and these two approximations shows greater scatter for the frozen-flow approximation than for the Zel'dovich approximation. The reason for these results is obvious. Our LEP approximation and the full gravitational simulation both produce high-density knots and filaments in the same general region of space. However, if the knots in one simulation are slightly displaced from the knots in the other simulation (as they are in these simulations), the result is that a high-density region in one simulation will lie on top of a low-density region in the other simulation, and vice versa, leading to a relatively low cross-correlation. On the other hand, the Zel'dovich approximation at late times produces a relatively diffuse distribution of matter in the high-density regions, so that the high-density regions in the gravitational clustering simulation are always correlated with a moderately high-density region in the Zel'dovich simulation. Our results and those of Matarrese et al. (1992), therefore, suggest that the cross-correlation, at least for unsmoothed density fields, is a questionable tool for comparing nonlinear evolution at late times; it is too sensitive to slight displacements in the high-density regions between two simulations. Whether such displacements represent a significant difference

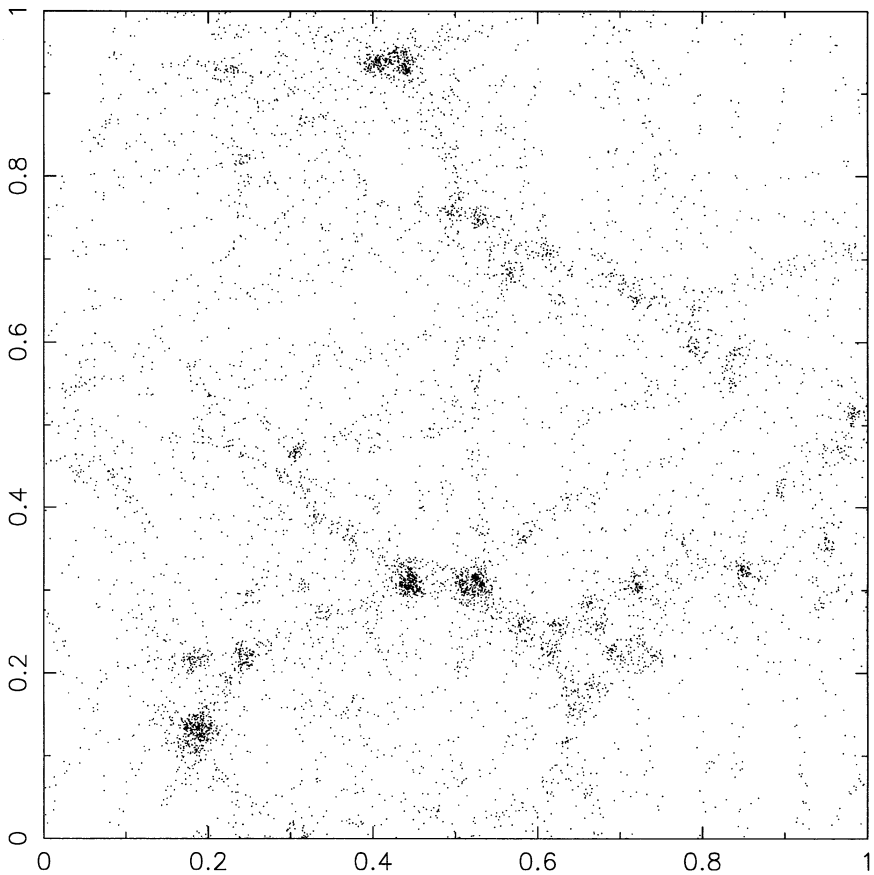


FIG. 4*a*

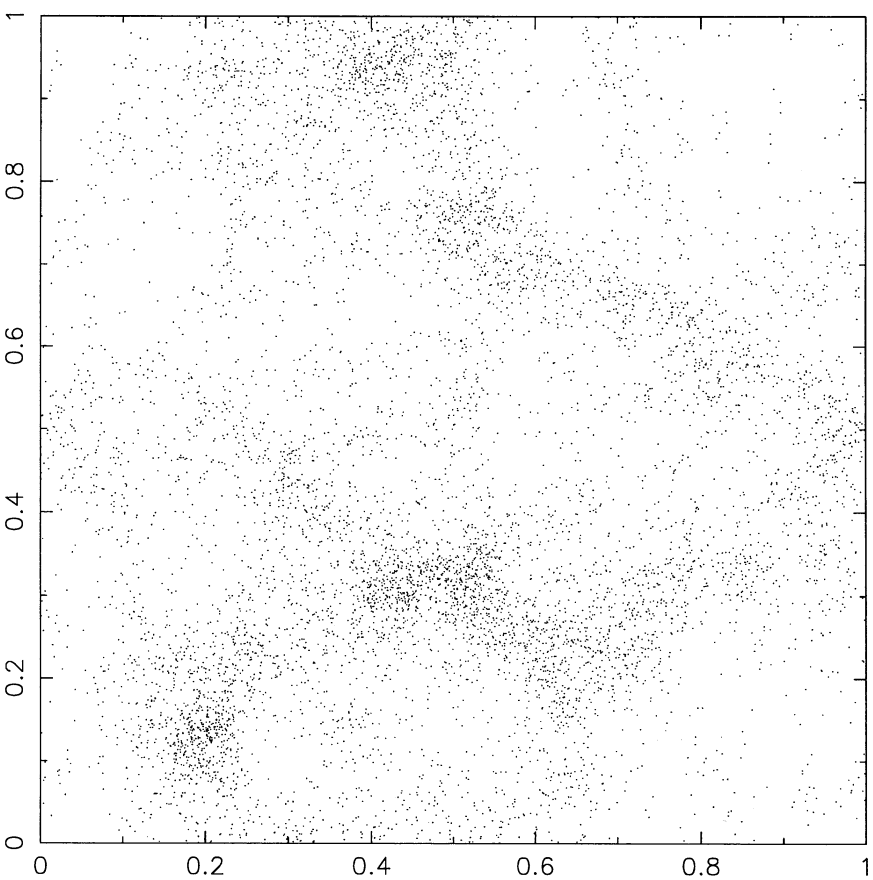


FIG. 4*b*

FIG. 4.—A slice of the universe 80 $h^{-1}$ Mpc × 80 $h^{-1}$ Mpc × 20 $h^{-1}$ Mpc, evolved to the present ($b = 1$) using $\Omega = 1$ Harrison-Zel'dovich adiabatic CDM initial conditions and (*a*) a full numerical (PM) simulation, (*b*) the Zel'dovich approximation, and (*c*) the linear evolution of the potential approximation.

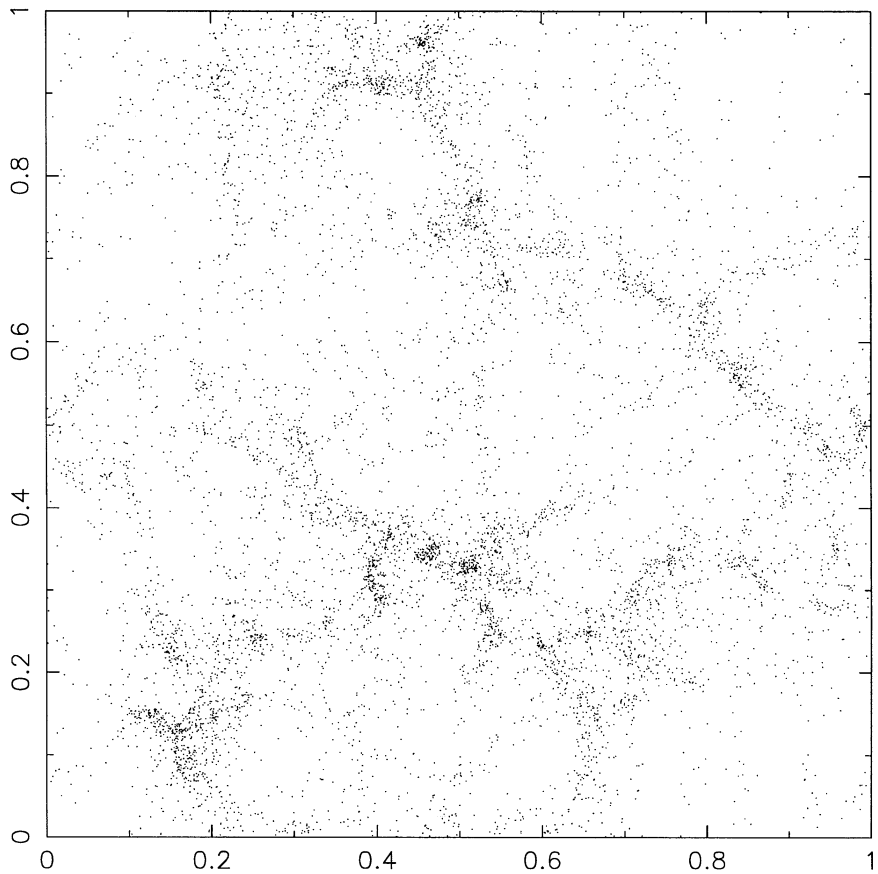


FIG. 4c

between density fields is obviously a matter of interpretation. This problem was noted by Coles et al. (1992).

Although the two-point correlation function uses only a small fraction of the total information in the density field, it confirms what is obvious visually. In Figure 5, we give the two-point correlation function $\xi(r)$ for our LEP approximation, the Zel'dovich approximation, and the full gravitational clustering simulation at various epochs. At late times ($b = 1.3$–1), the LEP approximation gives a two-point function which is much closer to the two-point function in the full gravitational clustering simulation than is the Zel'dovich two-point function. The LEP approximation and the gravitational clustering simulation produce two-point functions with similar slopes, although the LEP approximation gives a lower amplitude for $\xi$. The two-point function in the Zel'dovich approximation deviates strongly from the gravitational clustering two-point function at small scales.

We can also derive a number of interesting analytic results using the LEP approximation. Following Kofman (1991) and Matarrese et al. (1992), we note that equations (2.2)–(2.4) can be rewritten (for an $\Omega = 1$ matter-dominated universe) in terms of the variables $\eta = 1 + \delta$, $\boldsymbol{u} = d\boldsymbol{x}/da$, and $\varphi = (3/2)a^{-3}t^2\phi$:

$$\frac{d\boldsymbol{u}}{da} + \frac{3}{2a}\boldsymbol{u} = -\frac{3}{2a}\nabla\varphi\,, \tag{2.8}$$

$$\frac{d\eta}{da} + \eta\nabla\cdot\boldsymbol{u} = 0\,, \tag{2.9}$$

$$\nabla^2\varphi = \frac{\delta}{a}\,. \tag{2.10}$$

In both the frozen-flow approximation and our LEP approximation, the potential field is constant and is given by its initial linear value: $\varphi(\boldsymbol{x}, a) = \varphi_0(\boldsymbol{x})$. The frozen-flow approximation then takes the velocity $\boldsymbol{u}$ to be given by its linear value: $\boldsymbol{u}(\boldsymbol{x}, a) = -\nabla\varphi_0(\boldsymbol{x})$, while the LEP approximation uses equation (2.8) with $\varphi = \varphi_0$ to determine $\boldsymbol{u}$.

Suppose that a particle has Lagrangian coordinate $\boldsymbol{q}$, and its Eulerian position at scale factor $a$ is $\boldsymbol{x}(\boldsymbol{q}, a)$. Then equation (2.8) can be integrated to give the velocity $\boldsymbol{u}$ at Eulerian coordinate $\boldsymbol{x}$ at scale factor $a$. Without any approximation, we get

$$\boldsymbol{u}(\boldsymbol{x}, a) = -\frac{3}{2}a^{-3/2}\int_{a'=a_0}^{a}(a')^{1/2}\nabla\varphi[\boldsymbol{x}(\boldsymbol{q}, a'), a']da'\,, \tag{2.11}$$

where this integral (and the subsequent integrals in equations [2.12]–[2.16]) are taken over the trajectory $\boldsymbol{x}(\boldsymbol{q}, a')$ of the particle between $a_0$ and $a$. The LEP approximation then gives

$$\boldsymbol{u}(\boldsymbol{x}, a) = -\frac{3}{2}a^{-3/2}\int_{a'=a_0}^{a}(a')^{1/2}\nabla\varphi_0[\boldsymbol{x}(\boldsymbol{q}, a')]da'\,. \tag{2.12}$$

Equation (2.12) can be integrated by parts to show more clearly the relation between our LEP approximation and linear theory:

$$\boldsymbol{u}(\boldsymbol{x}, a) = -\nabla\varphi_0(\boldsymbol{x}) + \int_{a'=a_0}^{a}(a'/a)^{3/2} \times \{\boldsymbol{u}[\boldsymbol{x}(\boldsymbol{q}, a')]\cdot\nabla\}\nabla\varphi_0[\boldsymbol{x}(\boldsymbol{q}, a')]da'\,, \tag{2.13}$$

where we have taken $a \gg a_0$. The first term in equation (2.13) is the usual linear expression for the velocity, while the second term gives the deviation from linear theory in our LEP approx-

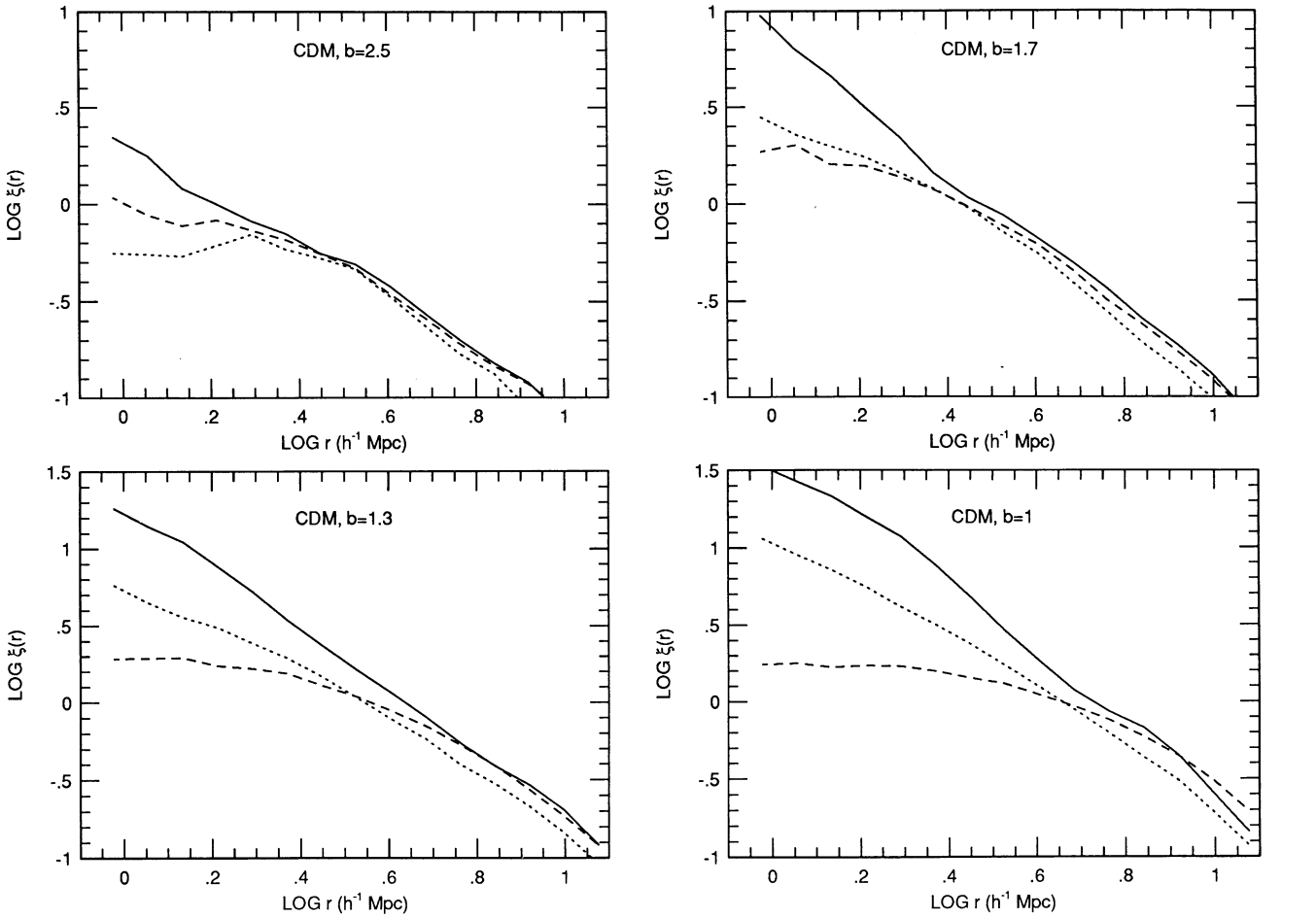


FIG. 5.—The two-point correlation function $\xi(r)$ for the CDM Harrison-Zel'dovich models of Fig. 4 using a full gravitational clustering simulation (*solid curve*), the Zel'dovich approximation (*dashed curve*), and the linear evolution of the potential approximation (*dotted curve*), at the indicated bias parameters $b$.

imation. In the frozen-flow approximation, $\boldsymbol{u}$ tracks its linear value $-\nabla\varphi_0$, and because $\varphi_0$ is Gaussian, so is $\nabla\varphi_0$, so the volume-weighted velocity distribution in the frozen-flow approximation is also Gaussian. Our LEP velocity distribution evolves away from a Gaussian because of the second term in equation (2.13).

We can also derive a formal expression for the density field in the LEP approximation by integrating equation (2.9) to derive the density $\eta$ at Eulerian coordinate $\boldsymbol{x}$ at scale factor $a$ (Matarrese et al. 1992):

$$\eta(\boldsymbol{x}, a) = \eta_0(q) \exp\left\{-\int_{\tilde{a}=a_0}^{a} \nabla\cdot\boldsymbol{u}[\boldsymbol{x}(\boldsymbol{q}, \tilde{a}), \tilde{a}]d\tilde{a}\right\}. \quad (2.14)$$

Using the LEP expression for $\boldsymbol{u}$ from equation (2.12), and changing the order of integration, we can perform the integral over $\tilde{a}$ to obtain:

$$\eta(\boldsymbol{x}, a) = \exp\left[\int_{a'=a_0}^{a} 3[1-(a'/a)^{1/2}]\delta_+[\boldsymbol{x}(\boldsymbol{q}, a')]da'\right], \quad (2.15)$$

where $\delta_+(\boldsymbol{x})$ is the (constant) value of $\delta(\boldsymbol{x})/a$ in the linear regime, and we have taken $\eta_0(q) \approx 1$. The corresponding expression for the frozen-flow approximation is (Matarrese et al. 1992)

$$\eta(\boldsymbol{x}, a) = \exp\left[\int_{a'=a_0}^{a} \delta_+[\boldsymbol{x}(\boldsymbol{q}, a')]da'\right]. \quad (2.16)$$

Both our LEP result and the frozen-flow result indicate that $\eta$ can be approximated as the exponential of an integral of the linear density field over the trajectory of the particle, but our result contains the additional weighting factor $3[1-(a'/a)^{1/2}]$. Thus, the LEP approximation gives more weight to the values of $\delta_+$ in the early part of the trajectory, and less weight to later values. For points which represent local minima or maxima of $\varphi_0$, the LEP approximation gives results identical to the frozen-flow approximation for $a \gg a_0$: $\boldsymbol{u} = 0$, and $\delta(\boldsymbol{x}, a) = \exp[\delta_+(\boldsymbol{x})a] - 1$. It is also easy to verify that for $a \gg a_0$, equation (2.15) produces a density contrast identical with the frozen-flow result for particle trajectories which are confined to regions in which $\delta_+$ is nearly constant.

Now we will provide a simple example to compare the predictions of our LEP approximation with the Zel'dovich approximation and the frozen-flow approximation. Consider the collapse of a spherical top hat perturbation, given by $\delta = \delta_0$ inside a radius $R$ embedded in a flat background. This problem was considered by Matarrese et al. (1992) for the frozen-flow approximation; here we extend the discussion to the LEP approximation. The potential is given by

$$\varphi_0(r) = \tfrac{1}{6}\delta_+ r^2, \quad (2.17)$$

where $r$ is the radial distance from the center of the potential well. Then $-\nabla\varphi_0 = -(\delta_+/3)r$. In our LEP approximation, we

can substitute equation (2.17) into equation (2.8) to obtain

$$\frac{d^2r}{da^2} + \frac{3}{2a}\frac{dr}{da} + \frac{1}{2a}\delta_+ r = 0 . \quad (2.18)$$

This equation is solved to yield:

$$r = [A \cos(\sqrt{2\delta_+ a}) + B \sin(\sqrt{2\delta_+ a})]a^{-1/2} , \quad (2.19)$$

where the constants $A$ and $B$ are chosen to give the correct initial position and velocity. For the growing mode with $r = r_0$ at $a = a_0$, in the limit where $a_0 \to 0$, we obtain:

$$r = r_0 \frac{\sin(\sqrt{2\delta_+ a})}{\sqrt{2\delta_+ a}} . \quad (2.20)$$

This solution can be compared with both the exact solution and the Zel'dovich and frozen-flow approximations. For example, for the growing mode in the exact solution, turnaround occurs at $a_{ta} = 1.06/\delta_+$ (where we take $a_0 \to 0$ throughout), compared with $a_{ta} = 1.5/\delta_+$ for the Zel'dovich approximation and $a_{ta} = 3/\delta_+$ for the frozen-flow approximation (Matarrese et al. 1992). The solution in equation (2.20) gives $a_{ta} = 2.06/\delta_+$ for the LEP approximation.

## 3. DISCUSSION

Our results from the full gravitational clustering code strongly support the hypothesis that the peculiar gravitational potential smoothed on 1.25 $h^{-1}$ Mpc scales is roughly constant down to the present (Fig. 2). Although we have examined only the $\Omega = 1$ Zel'dovich CDM model, any other model with a similar power spectrum should give a similar result. Hence, it is not surprising that our LEP (linear evolution of the potential) approximation, in which the potential is held constant and the matter evolves according to the standard equations of motion in this potential, produces results in good agreement with an exact numerical simulation. Our result for the evolution of the potential also provides support for the frozen-flow approximation (Matarrese et al. 1992), in which both the peculiar potential and peculiar velocity are given by their linear values. Our LEP approximation is more exact than the frozen-flow approximation, but at the expense of greater computational complexity. Both the LEP and frozen-flow approximations give much better results far into the nonlinear regime than does the Zel'dovich approximation. The frozen-flow and LEP approximations are both natural generalizations of the Zel'dovich approximation, in which the Eulerian potential, rather than the Lagrangian potential, is held constant. With respect to accuracy and computational complexity, the LEP approximation lies between the frozen-flow approximation and a full gravitational clustering simulation.

The peculiar gravitational potential is constant only for $\Omega = 1$ models, and our results are valid only for such models. However, it would be easy to extend the LEP approximation to $\Omega < 1$ models by simply scaling the initial potential at every time step by the appropriate amount. From equation (2.4), $\phi$ is proportional to $\delta/a$ in the linear regime. Thus, linear evolution of the potential simply involves multiplying the initial value of $\phi$ by $D/a$ at any later time, where $D$ is the growth factor in linear perturbation theory. For $z \gg \Omega^{-1}$ this factor is unity, while for $z \ll \Omega^{-1}$ it decreases as $a^{-1}$.

Our numerical gravitational clustering results indicate no obvious correlation between the initial and final values of the density field measured at a fixed point (Fig. 1). This argues against the usefulness of any local models for the density evolution, in which the final density field is expressed as a function of the initial density field (e.g., the lognormal model of Coles & Jones 1991). The correlation between the initial and final density fields on 1.25 $h^{-1}$ Mpc scales appears to break down near $b = 6$. Weinberg (1992) has argued that weakly nonlinear evolution should preserve the rank ordering of the density field (smoothed on an appropriate scale), i.e., if $\delta(\boldsymbol{x}_1) > \delta(\boldsymbol{x}_2)$ in the linear regime, then we expect $\delta(\boldsymbol{x}_1) > \delta(\boldsymbol{x}_2)$ in the weakly nonlinear regime. Our results in Figure 1 indicate that this argument is roughly valid on 1.25 $h^{-1}$ Mpc scales down to $b = 10$, but it begins to fail near $b = 6$. These results are not directly applicable to Weinberg's work, since he examined density fields smoothed on somewhat larger length scales. Our analytic results in the LEP approximation indicate that the evolved density field can be expressed as an integral of the linear density field over the path of the particle, similar to the result obtained in the frozen-flow approximation.

Our LEP approximation reduces the computational time needed to evolve a density field. We find that the LEP approximation requires one-fifth the CPU time of a full PM code for the parameters used here. This improvement was obtained by simply overriding the calculation of the potential in the PM code of Villumsen (1989); a dedicated LEP code might be even faster. If $N$ is the number of particles and the number of grid cells in the simulation, then the calculation of the potential is roughly an $N \log N$ operation (in the limit of large $N$), while the LEP algorithm simply goes as $N$. Thus, we expect an even larger speed-up factor for larger simulations. The LEP approximation has several other potential advantages. If the initial potential can be specified analytically, then the LEP approximation can be made gridless, and such a simulation might be useful for hydrodynamic simulations prior to the formation of shocks. In principle, an arbitrarily large number of particles can be used in the LEP approximation, since there is no need to calculate their evolution simultaneously. The LEP approximation can also be used for studying the fate of a small fraction of the matter in the simulation without evolving the full matter field; in this case a large number of particles could be evolved in a small region of space to get better resolution.

In addition to these numerical advantages, the LEP approximation can provide a better analytic understanding of gravitational clustering. We have derived a number of analytic results and in particular have obtained an expression for the deviation of the velocity field from its linear value. Further analytic results should be obtainable.

After this paper was submitted, we learned of very similar work done independently by Bagla & Padmanabhan (1993). They performed a number of two-dimensional simulations comparing the LEP approximation with both the frozen-flow and Zel'dovich approximation and argued that it is superior to both.

We thank M. Strauss for helpful comments on the manuscript. R. J. S. was supported in part by the DOE (DE-AC02-76ER01545) and by NASA (NAGW-2589). J. V. V. and T. G. B. were supported in part by the NSF (AST 89-21001). T. G. B. was supported by a Presidential Fellowship at The Ohio State University and by the NSF (AST 89-13664 and AST 89-17765) at Caltech. The numerical simulations were run on the CRAY Y/MP at the Ohio Supercomputer Center.

REFERENCES

Bagla, J. S., & Padmanabhan, T. 1993, MNRAS, submitted
Bardeen, J. M., Bond, J. R., Kaiser, N., & Szalay, A. S. 1986, ApJ, 304, 15
Coles, P., & Jones, B. 1991, MNRAS, 248, 1
Coles, P., Melott, A. L., & Shandarin, S. R. 1993, MNRAS, 260, 765
Efstathiou, G., Davis, M., Frenk, C. S., & White, S. D. M. 1985, ApJS, 57, 241
Gramann, M. 1993, ApJ, 405, L47
Gurbatov, S. N., Saichev, A. I., & Shandarin S. F. 1989, MNRAS, 236, 385
Kofman, L. 1991, in Primordial Nucleosynthesis and Evolution of Early Universe, ed. K. Sato & J. Audouze (Dordrecht: Kluwer), 495
Matarrese, S., Lucchin, F., Moscardini, L., & Saez, D. 1992, MNRAS, 259, 437
Nusser, A., & Dekel, A. 1992, ApJ, 391, 443
Peebles, P. J. E. 1980, The Large-Scale Structure of the Universe (Princeton Univ. Press)
Villumsen, J. V. V. 1989, ApJS, 71, 407
Weinberg, D. H. 1992, MNRAS, 254, 315
Zel'dovich, Ya. B. 1970, A&A 5, 84